Metallophysics and Advanced Technologies
Металофіз. новітні технол.
Metallofiz. Noveishie Tekhnol.
2024, vol. 46, No. 8, pp. 797–810
https://doi.org/10.15407/mfint.46.08.0797
Reprints available directly from the publisher

PACS numbers: 64.70.D-, 64.70.dg, 64.70.dj, 81.30.Fb, 81.40.Ef, 82.40.Ck, 82.60.Lf

Fast Melting and Crystallization of Interfaces in Eutectic Alloys —The Idea of 'Thermal Prick'

S. Abakumov[**], A. Titova[*,**], and A. M. Husak[*,**]

[*]*Ensemble3 Centre of Excellence,*
Wolczynska Str. 133,
01-919 Warsaw, Poland
[**]*Bohdan Khmelnytsky National University of Cherkasy,*
81 Shevchenko Blvd.,
UA-18031 Cherkasy, Ukraine

The possibility of nanomodification of eutectic alloys by fast heating slightly above eutectic temperature with subsequent very fast cooling or just quenching is analysed. The basic physical effect that may be a basis of such a 'thermal prick' idea is the following: (1) short-time contact melting of any interphase interface leads to the formation of a thin liquid layer instead of a parent solid–solid interface; (2) fast cooling of this thin liquid layer proceeds under the step of composition between opposite boundaries. Therefore, the phase transformation should be in an open inhomogeneous system. In many cases, crystallization is reduced to decomposition under the external composition gradient and demonstrates quasi-periodic phase formation with nanometre separation distance. It means that the special heat treatment, which we call the thermal prick, may create additional nanostructured zones around each interface within the parent eutectic alloy.

Key words: eutectic alloy, contact melting, crystallization, diffusion, kinetics, nanostructure.

Проаналізовано можливість наномодифікування евтектичних стопів швидким нагріванням трохи вище евтектичної температури з подальшим дуже швидким охолодженням або просто загартуванням. Основний фізичний ефект, який може бути покладений в основу такої ідеї «термічного

Corresponding author: Andriy Mykhaylovych Husak
E-mail: amgusak@ukr.net

Citation: S. Abakumov, A. Titova, and A. M. Husak, Fast Melting and Crystallization of Interfaces in Eutectic Alloys—The Idea of 'Thermal Prick', *Metallofiz. Noveishie Tekhnol.*, **46**, No. 8: 797–810 (2024). DOI: 10.15407/mfint.46.08.0797

уколу», полягає в наступному: (1) короткочасне контактне топлення будь-якої міжфазної межі поділу евтектичної системи приводить до утворення тонкого рідкого шару замість материнської поверхні поділу між твердими фазами; (2) швидке охолодження цього тонкого рідкого шару відбувається в умовах зовнішнього ґрадієнту концентрації між протилежними стінками прошарку. У багатьох випадках кристалізація зводиться до розпаду у полі зовнішнього ґрадієнту концентрації та демонструє квазіперіодичне фазоутворення з нанометровими періодами. Це означає, що спеціяльне термічне оброблення, яке ми називаємо термічним уколом, може створювати додаткові наноструктуровані зони навколо кожної межі поділу у материнському евтектичному стопі.

Ключові слова: евтектичний стоп, контактне топлення, кристалізація, дифузія, кінетика, наноструктура.

(Received 15 February, 2024; in final version, 6 May, 2024)

1. INTRODUCTION

In this paper, we try to combine the simple engineering idea (suggestion of thermal prick method for the heat treatment of the eutectic alloys) with the fundamental concept of phase transformations in open non-uniform systems.

1.1. Idea of Thermal Spike Method

During the last two decades, eutectic alloys have been more and more applied not only as solders but as well as self-organized two-phase or multiphase materials in photonics, energy storage, and conversion [1–9]. For many such applications, a fraction of internal interphase surfaces becomes important. Therefore, it might be interesting for practice to have the ability to increase the total interphase surface of already produced eutectic alloys. We may call our aim 'the nanomodification of structure'. If eutectic alloy is produced by directional crystallization (for example, by the 'micropulling-down' method), it often demonstrates lamellar or rod-like structures [7–10]. At that, typical diameters of rods or thicknesses of lamellae of the primary phase have the order of few microns, as well as distances between rods or lamellae. In short, the main idea is to apply to such alloys a special regime of heat treatment, which we call a 'thermal prick (spike)'—fast heating over the eutectic temperature (but below the melting points of both phases of the eutectic couple) for some short time, and then, fast cooling (or just quenching). One might expect that during heating over eutectic temperature the partial melting of the eutectic alloy should start. (We emphasize that the aim of the thermal prick (spike) is not complete but only partial melting with remaining significant regions of alloy in the

solid state.) Theoretically, above the eutectic temperature, contact melting should start at each internal interphase interface after some nucleation period (nucleation of the first liquid droplet), which we expect to be short [11]. According to the idea of a 'thermal prick', if the time of this local melting is short enough, we can convert all (or a significant part of) interfaces into such liquid layers with a concentration gradient inside the molten layer when the thickness of this layer (say, 500 nm or 1 micron) is less than the size of single-phase regions. When, after this short period of growth, these molten layers crystallize back during fast cooling, they may form additional nanosize two-phase structures around each 'parent' internal interface. Recently, we discovered the formation of the quasi-periodic spinodal-type nanostructure within the region of the liquid layer in the sharp concentration gradient for eutectic systems like Cu–Ag [11]. This system has the same type of lattice for both components and has a decomposition cupola with a critical temperature above eutectic. This leads to an interesting interplay of eutectic and spinodal decomposition.

So, our working hypothesis is to apply the fast heating above eutectic temperature (but below melting temperatures of components) followed by fast cooling. Such thermal spike may convert each internal interphase interface of the eutectic alloy into micron-sized or submicron-sized nanostructured layers consisting of alternating nanolayers of both phases or just from a mixture of nanograins of both phases. Thus, the area of interphase surfaces will grow significantly.

1.2. Crystallization of thin Molten Layer between Different Phases as a Problem of Decomposition in an Open Non-Uniform System

Crystallization of narrow molten alloy between different phases at the 'left' and 'right' boundaries is, actually, the phase transformation in an open inhomogeneous system (under external gradient of compositions and chemical potentials and/or external flux of matter and/or energy). We may call such systems 'driven' (following the terminology of Georges Martin *et al.* [12–14]). Development of such an approach for the case of flux-driven nucleation, growth, and ripening in open systems can be found in Refs. [15, 16]. Decomposition in open inhomogeneous systems has been analysed so far only partially. Actually, decomposition may be of spinodal type, precipitation-and-growth type, and cellular-decomposition-*via*-moving-boundaries type under frozen bulk diffusion. So far, we have analysed and compared with experiment only flux-driven cellular decomposition [17–19] for various systems. Spinodal decomposition in an open system has been partially analysed recently [11] and is analysed and simulated with more details below. Decomposition by precipitation-growth in an open system is simulated below for the first time (to the best of our knowledge).

1.3. Structure of the Paper

First, we will model the first stage of thermal spike processing—contact melting of internal interfaces within the eutectic alloy (Sec. 2). Let the interface between the two phases be locally planar, and the temperature slightly (by several degrees) above the eutectic one. In general, contact melting includes three stages. The first stage is a nucleation of the first droplets. The second stage is a lateral growth of the liquid phase along the interface with the formation of a continuous liquid layer. The third (final) stage is the normal growth of the formed thin liquid phase layer due to the fast diffusion of components across this layer from one solid phase to another. For nucleation-stage estimation, we use the recently developed theory of nucleation in contact melting (see Ref. [11]). The lateral spreading stage is typically very short. The normal growth stage is described in Sec. 2 according to the common description of reactive diffusion.

In Section 3, we try to model the more complicated phenomenon—crystallization of the liquid interface layer between two members of the eutectic couple. This crystallization may proceed via various modes, depending on system type and kinetic factors.

We will analyse two types of systems. The first type is a eutectic couple of the Cu–Ag-type, which has the same structure of both components, positive mixing energy, and decomposition cupola with the top (critical temperature) higher than the eutectic one (Fig. 1). It means that, below the eutectic temperature, the liquid alloy may crystallize as minimum via two modes: (1) by nucleation and growth of the primary phase and the secondary phase, and (2) by a two-step process, consisting of, first, polymorphic (at frozen long-range diffusion) freezing into solid solution, which is unstable in respect to spinodal decomposition, and (second) this very spinodal decomposition and consequent coarsening.

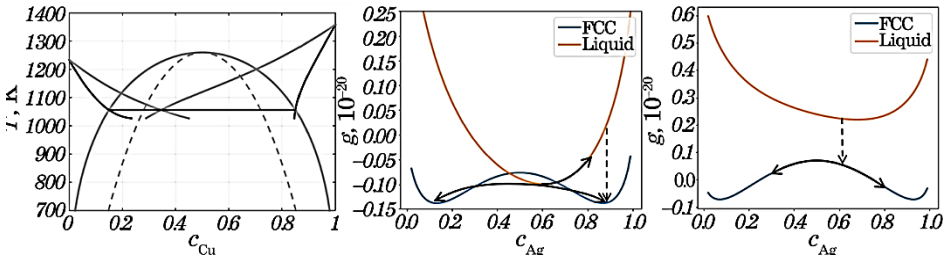

Fig. 1. In the case of the Cu–Ag system, the second mode (polymorphous freezing into an unstable solid solution that decomposes spinodal into two solid solutions) was predicted [11] to become preferential at $T < 970$ K, which is not very far from eutectic and should become realistic with fast cooling.

The second mode of crystallization of the first-type systems becomes preferential at fast cooling below some threshold temperature, at which the W-curve of the solid solution becomes lower than the g-curve of the liquid phase [11].

Systems of the second type contain several intermediate ordered phases (compounds) with narrow concentration ranges. They are characterized by negative mixing energy for interactions within the first coordination shell (and, possibly though not necessary, positive mixing energy with the second coordination shell). Such a system tends to an ordering within narrow concentration ranges around stoichiometric compounds, and decomposition into two ordered compounds $AB + A_3B$, or rather one compound and one marginal solid solution $A_3B + A$, beyond the mentioned concentration ranges.

Namely, we will limit ourselves to two kinds of structural phase transformations forming the f.c.c. lattice: (1)—decomposition into two solid solutions, (2) decomposition into solid solution plus ordered compound $L1_2$, and (3) decomposition into two different ordered compounds $L1_2$ and $L1_0$—see Fig. 2, *b*.

2. ESTIMATION OF TIME NECESSARY TO CONVERT SOLID INTERFACE INTO A MOLTEN LAYER OF NECESSARY THICKNESS VIA CONTACT MELTING

We want to melt the interfaces between two phases with the formation of liquid layers at the base of each interface. The thickness of the liquid layer should be less than the thickness of alpha and beta lamellae or rods. Moreover, maximal temperature of the thermal prick should be higher than the eutectic one but lower than the melting of pure components. As mentioned in the Introduction, contact melting should start from nucleation in concentration gradients within parent solid phases, due to interpenetration of components within the contact zone. For the case of Cu–Ag contact melting, the threshold interpenetration zone is about 10–20 nm and the time for its formation by solid-state diffusion may be (under reasonable nucleation conditions and parameters) a few milliseconds. We will see that the characteristic time of normal growth, necessary to reach a liquid layer thickness of about a micron, is about one or a few seconds. Therefore, in what follows below, we neglect the nucleation time of the liquid phase at the beginning of contact melting. Then, the kinetics of widening of the molten layer can be described by the following equations of mass balance at the moving interfaces Y^R (between liquid layer and BETA-phase) and Y^L (between liquid layer and ALPHA-phase):

$$\left(C_{beta} - C^R_{melt}\right)\frac{dY^R}{dt} = D_{melt}\,\frac{C^R_{melt} - C^L_{melt}}{Y^R - Y^L}, \qquad (1)$$

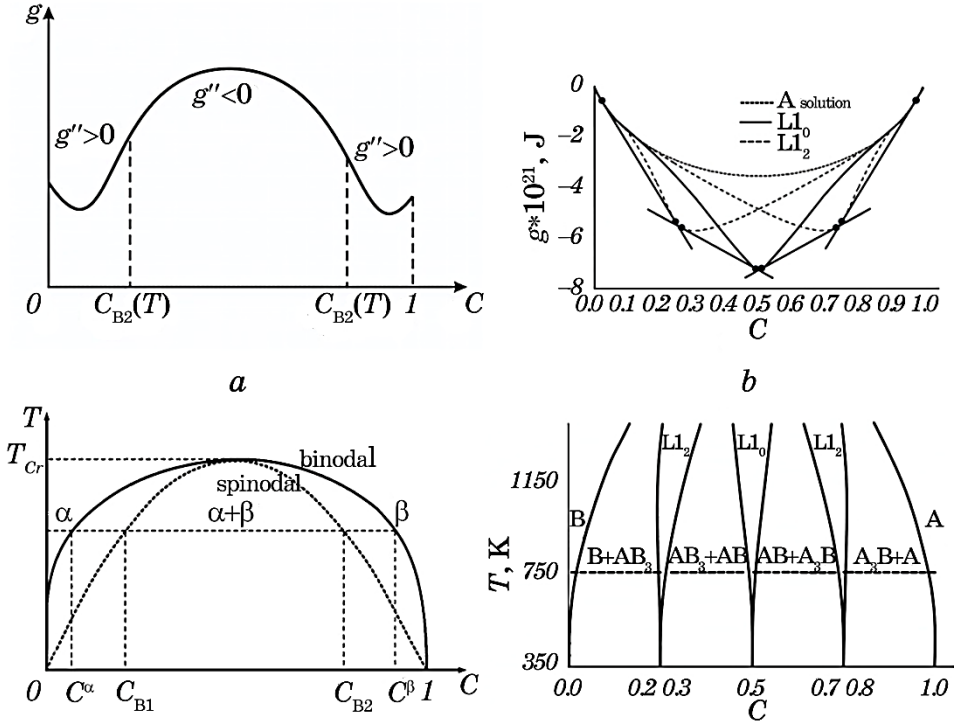

Fig. 2. Two types of binary systems analysed in this paper, characterized by (up) composition dependencies of Gibbs free energy and (bottom) phase diagrams: *a*—positive mixing energy and corresponding *W*-shaped *g*(*C*)-curve leading to decomposition into two solid solutions (at least in the bulk if the bulk diffusion is not frozen), *b*—negative mixing energy for the nearest neighbours and positive mixing energy for the next nearest neighbours, leading to the ordering of compounds within narrow concentration ranges around 1/4, 1/2, 3/4, and leading to decomposition into A_3B compound + A(B) solution or A_3B compound + AB compound, *etc*., beyond the mentioned narrow ranges.

$$\left(C^{L}_{melt} - C_{alpha}\right)\frac{dY^{L}}{dt} = -D_{melt}\frac{C^{R}_{melt} - C^{L}_{melt}}{Y^{R} - Y^{L}}, \tag{2}$$

$$C^{R}_{melt} \approx C_{eut} + \frac{\left(T - T_{eut}\right)}{\partial T^{R}_{liq} / \partial C}, \qquad \frac{\left(T - T_{eut}\right)}{\partial T^{R}_{liq} / \partial C} << C_{eut},$$

$$C^{L}_{melt} \approx C_{eut} + \frac{\left(T - T_{eut}\right)}{\partial T^{L}_{liq} / \partial C}, \qquad -\frac{\left(T - T_{eut}\right)}{\partial T^{L}_{liq} / \partial C} << C_{eut},$$

$$C^{R}_{melt} - C^{L}_{melt} \approx +\frac{\left(T - T_{eut}\right)}{\partial T^{R}_{liq} / \partial C} - \frac{\left(T - T_{eut}\right)}{\partial T^{L}_{liq} / \partial C} = \left(\frac{1}{\partial T^{R}_{liq} / \partial C} + \frac{(-1)}{\partial T^{L}_{liq} / \partial C}\right)\left(T - T_{eut}\right). \tag{3}$$

According to the phase diagram and our rough estimations for Ag–Cu system (see Fig. 3),

$$\partial T_{liq}^{R} / \partial C - \partial T_{liq}^{L} / \partial C \approx 0.0004,$$

$$d\left(\Delta Y_{melt}\right)^2 = 2D_{melt}\left(\frac{C_{beta} - C_{alpha}}{\left(C_{beta} - C_{eut}\right)\left(C_{eut} - C_{alpha}\right)}\right) \cdot 0.004 \cdot \left(T - T_{eut}\right) dt\,, \quad (4)$$

$$t_{melt} = \frac{\left(\Delta Y_{melt}\right)^2}{2D_{melt}\left(\frac{C_{beta} - C_{alpha}}{\left(C_{beta} - C_{eut}\right)\left(C_{eut} - C_{alpha}\right)}\right) \cdot 0.004 \cdot \left(T - T_{eut}\right)}. \quad (5)$$

If, say, $\Delta Y_{melt} = 2 \cdot 10^{-6}$ m, $D_{melt} = 0.5 \cdot 10^{-9}$ m^2/s, $C_{alpha} = 0.1$, $C_{eut} = 0.95$, $T - T_{eut} = 2$ K, then, $t_{melt} \approx 0.1$ sec .

So, if we keep the interface at a temperature of 2 K higher than eutectic for about 0.1 seconds, it may convert into a liquid layer of a thickness of 2 microns, of course, if nucleation of the liquid phase proceeds even faster.

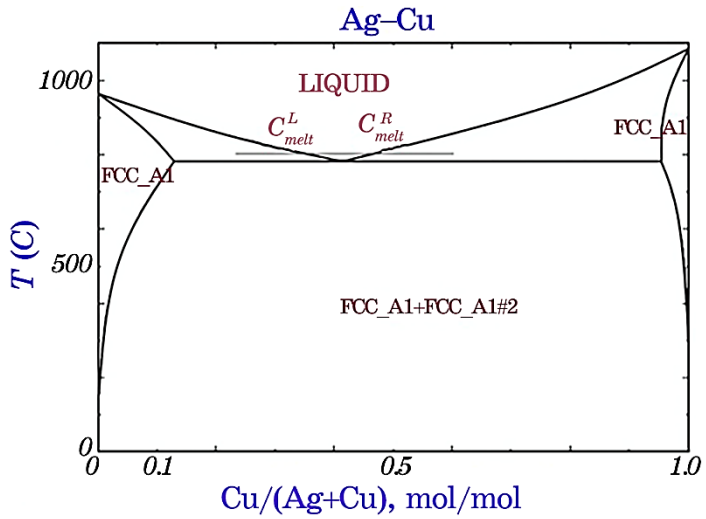

Fig. 3. Typical phase diagram of the eutectic couple. At temperature T slightly above eutectic one, T_{eut}, the concentration range of the growing intermediate liquid phase is determined by the derivatives of the liquidus lines left and right of the eutectic point:

$$C_{melt}^{R} - C_{melt}^{L} \approx \left(\frac{1}{\partial T_{liq}^{R} / \partial C} + \frac{(-1)}{\partial T_{liq}^{L} / \partial C}\right)\left(T - T_{eut}\right).$$

3. CRYSTALLIZATION OF LIQUID LAYER BETWEEN THE COMPONENTS OF THE EUTECTIC SYSTEM

3.1. Crystallization of the First-Type Eutectic Interface Alloy

At first, we simulated the two-stage crystallization of the first type of alloy (Cu–Ag-type) under fast heating. We used a new simulation method Generalized Stochastic Kinetic Mean–Field (GSKMF) developed recently [11]. This method simulates simultaneously the time evolution of the liquid–solid order parameter, as well as the spatial redistribution of components. Results of the GSKMF application demonstrated [11] that the obtained morphology practically coincides with that obtained by simulation of spinodal decomposition in a solid state in an inhomogeneous open system—with fixed phases alpha and beta at the opposite sides of the crystallized layer. Therefore, here (below), instead of GSKMF, we use a more known simulation tool SKMF (Stochastic Kinetic Mean–Field in solid state) [20–27] for the calculation of occupation probabilities at the sites of rigid f.c.c. lattice. The typical result of such simulation for Ag–Cu is shown in Fig. 4 (left): quasi-periodic formation of several nanolayers along the former interface.

In Figure 4 (right), we demonstrate the result of spinodal decomposition at the same parameters but in a closed system with periodic boundary conditions. We see that the morphology of the crystallized eutectic layer strongly depends on the boundary conditions.

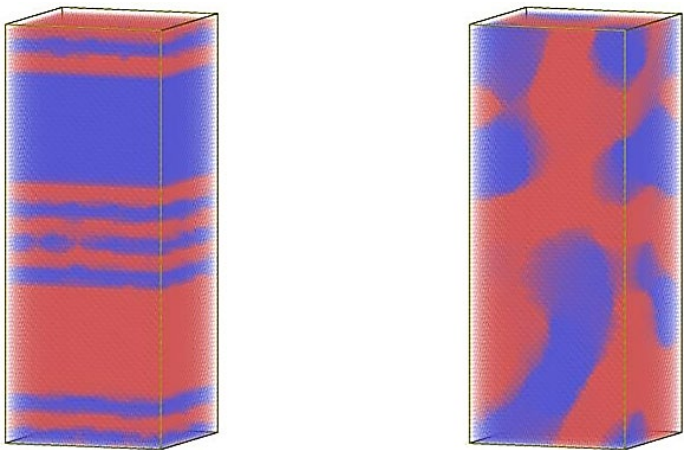

Fig. 4. Typical morphologies simulated for the case of a thermal prick of the interphase interface (left) and spinodal decomposition in homogeneous external conditions (right). In the first case, crystallization is reduced to spinodal decomposition in the open inhomogeneous system under differences in compositions and chemical potentials of two adjacent phases.

3.2. Crystallization of the Second-Type Eutectic Interface Alloy

System of the second type was also simulated by the SKMF method and was characterized by the following interaction energies within two coordination shells leading to the phase diagram shown in Fig. 2, *b*:

$$V_{AA}^{I} = V_{BB}^{I} = -10^{-21} J,\ V_{AB}^{I} = -3.9 \cdot 10^{-21} J\ ,$$
$$V_{AA}^{II} = V_{BB}^{II} = -8.76 \cdot 10^{-21} J,\ V_{AB}^{II} = -2 \cdot 10^{-21} J\ .$$

Peculiarities of the SKMF algorithm in the case of interactions within two shells were discussed recently [23]. Peculiarities of the description of the compounds A_3B and AB with local compositions and with so-called 'local long-range-order parameters' were explained also [22, 23]. Like in the previous subsection, instead of liquid, we took, as an initial state of quenched liquid, the random alloy at the f.c.c. rigid (already formed) lattice.

In parallel, we simulated the same system evolution with the same boundary conditions by the standard Monte Carlo method (exchange mechanism, Metropolis algorithm).

We considered two cases of initial states.

1. Random alloy with 0.125 fraction of B. This random alloy is unstable and should decompose into the ordered compound A_3B (with a composition close to stoichiometric one) and a weak solution of B in A.

2. Random alloy with 0.375 fraction of B. This random alloy is also unstable and should decompose into the ordered compound A_3B (structure $L1_2$ with a composition close to stoichiometric) and another ordered compound AB (structure $L1_0$ with a composition close to stoichiometric).

At that, we characterized each site by local mean concentration, averaged over this very site and 12 nearest neighbours:

$$C_{mean}\left(i\right) = \frac{C\left(i\right) + \frac{1}{4}\sum_{in=1}^{12} C\left(in\right)}{4}. \qquad (6)$$

In homogeneous ordered phases, this parameter remains the same for all sublattices in A_3B and AB compounds. Therefore, oscillations of C_{mean} indeed, demonstrate the quasi-periodic formation of phases instead of transitions between sublattices (see below).

3.2.1. System A–Frozen Solution–A_3B

The initial state was, from one side, 50 (001)-planes of almost pure A, from another side—50 (001)-planes of almost stoichiometric ordered phase A_3B (structure $L1_2$), 200 (001)-planes between them are filled

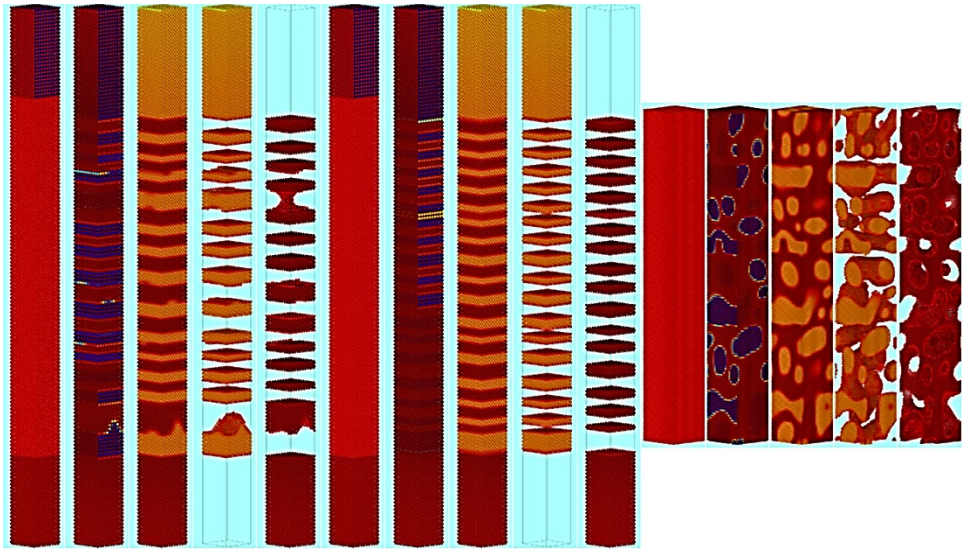

Fig. 5. Patterns after crystallization and decomposition into $A + A_3B$ of molten interface, in comparison with decomposition in closed system:
a) initial noise = 1%, A—bottom, A_3B—top;
b) initial noise = 0%, A—bottom, A_3B—top;
c) initial noise = 0%, periodic boundary conditions (closed system).
KMF method, composition scales with colour:
Column 1—initial state, colour corresponds to actual composition of each site;
Column 2—state after 150000 time steps, colour corresponds to actual composition;
Column 3—state after 150000 time steps, colour corresponds to C_{mean};
Column 4—state after 150000 time steps, sites with $C_{mean} > 0.125$;
Column 5—state after 150000 time steps, sites with $C_{mean} < 0.125$.

with random alloy with atomic fraction 0.125 of B. In KMF simulations, it is realized with just the same (or in some cases with small initial noise) occupation probability at each site (Fig. 5). In Monte Carlo simulations, we randomly filled sites by sort A or B with respective probabilities 0.875 and 0.125 (Fig. 7, *a*).

3.2.2. System A_3B–Frozen Solution–AB

Similar results have been obtained for the random alloy at the interface between two ordered compounds A_3B and AB—quasi-periodic patterns are formed, contrary to a closed system with periodic boundary conditions (Fig. 6).

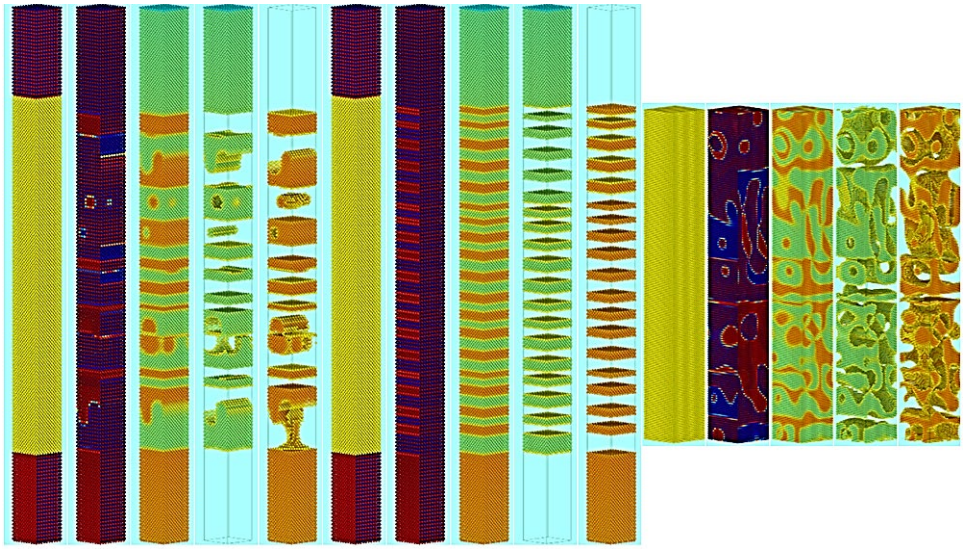

Fig. 6. Patterns after crystallization and decomposition into $A_3B + AB$ of molten interface, in comparison with decomposition in closed system:
a) initial noise = 1%, A_3B—bottom, AB—top;
b) initial noise = 0%, A_3B—bottom, AB—top;
c) initial noise = 0%, periodic boundary conditions (closed system).
KMF method, composition scales with colour:
Column 1—initial state, colour corresponds to actual composition of each site;
Column 2—state after 150000 time steps, colour corresponds to actual composition;
Column 3—state after 150000 time steps, colour corresponds to C_{mean};
Column 4—state after 150000 time steps, sites with $C_{mean} > 0.375$;
Column 5—state after 150000 time steps, sites with $C_{mean} < 0.375$.

3.2.3. Monte Carlo Simulation of the Systems 'A–Frozen Solution–A_3B' and 'A_3B–Frozen Solution–AB'

We simulated the decomposition of the random solution layer between two walls of adjacent parent phases, as well, by Monte Carlo method, using the simplest Metropolis algorithm with exchange mechanism. As can be seen in Fig. 7, the results also show the formation of some quasi-periodic pattern.

4. CONCLUSIONS

We suggest a simple method of nanostructuring the eutectic alloys by special heat treatment, which we call a 'thermal prick (spike)': the fast

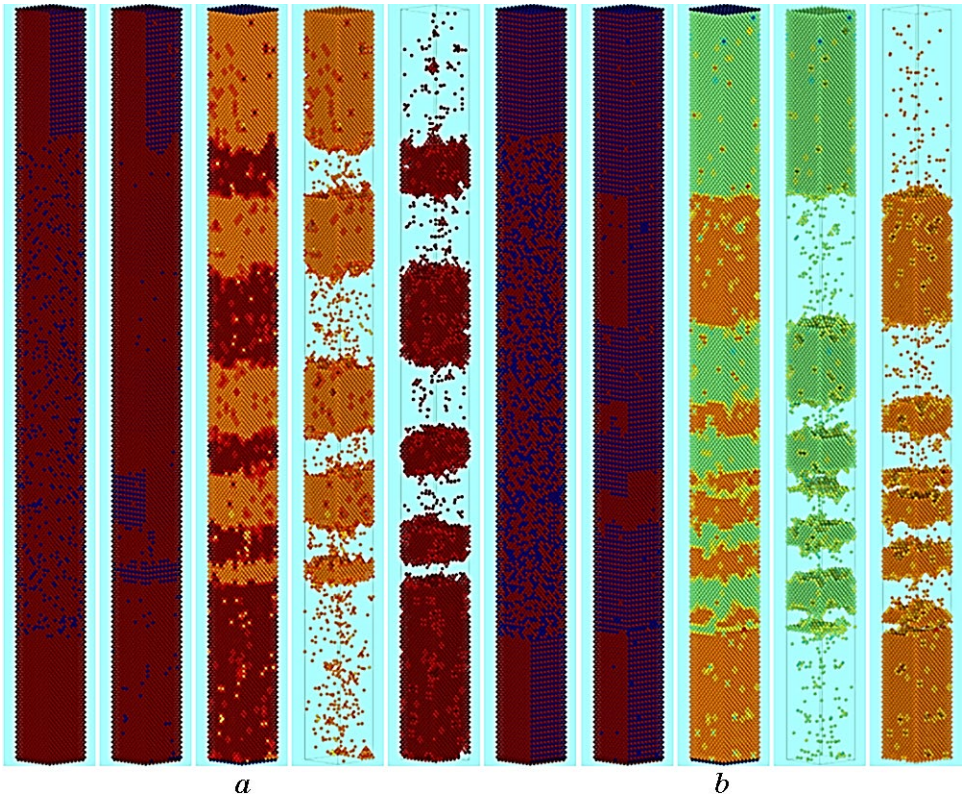

Fig. 7. Patterns after crystallization and decomposition into $A+A_3B$ (left) and A_3B+AB (right) of molten interface, in comparison with decomposition in closed system.
Monte Carlo method.
Column 1—initial state, colour corresponds to actual composition of each site;
Column 2—state after 150000 time steps, colour corresponds to actual composition;
Column 3—state after 150000 time steps, colour corresponds to C_{mean};
Column 4—state after 150000 time steps, sites with $C_{mean} > 0.125$ (left) and sites with $C_{mean} < 0.125$ (right);
Column 5—state after 150000 time steps, sites with $C_{mean} > 0.375$ (left) and sites with $C_{mean} < 0.375$ (right).

heating to temperatures a few degrees above the eutectic one and fast cooling (quenching). This treatment should generate partial internal contact melting of the interfaces with subsequent crystallization in the non-uniform conditions leading to the formation of additional nanostructures around these interfaces.

Fast heating, depending on the system, may be realized by passing

current, laser pulse, inertial passing through the heating zone, *etc*.

Authors are grateful to Dorota Pawlak, Kingshuk Bandopadhyay, Jaroslaw Sar, and Yaroslav Korol for discussion of thermal-spike idea.

This work was supported by the ENSEMBLE3 Project (MAB/2020/14), which is carried out within the International Research Agendas Programme (IRAP) of the Foundation for Polish Science co-financed by the European Union under the European Regional Development Fund and the Teaming Horizon 2020 program [GA #857543] of the European Commission.

REFERENCES

1. Yu. Taran and V. Mazur, *Struktura Evtekticheskikh Splavov* (Moskva: Metallurgiya: 1978) (in Russian).
2. D. A. Pawlak, K. Kolodziejak, S. Turczynski, J. Kisielewski, K. Rozniatowski, R. Diduszko, M. Kaczkan, and M. Malinowski, *Chem. Mater.*, **18**, Iss. 9: 2450 (2006).
3. K. Sadecka, M. Gajc, K. Orlinski, H. B. Surma, A. Klos, I. Jozwik-Biala, K. Sobczak, P. Dluzewski, J. Toudert, and D. A. Pawlak, *Adv. Opt. Mater.*, **3**, Iss. 3: 381 (2015).
4. K. Wysmulek, J. Sar, P. Osewski, K. Orlinski, K. Kolodziejak, A. Trenczek-Zajac, M. Radecka, and D. A. Pawlak, *Appl. Catal., B*, **206**, 538 (2017).
5. D. A. Pawlak, S. Turczynski, M. Gajc, K. Kolodziejak, R. Diduszko, K. Rozniatowski, J. Smalc, and I. Vendik, *Adv. Funct. Mater.*, **20**, Iss. 7: 1116 (2010).
6. P. Osewski, A. Belardini, M. Centini, C. Valagiannopoulos, G. Leahu, R. Li Voti, M. Tomczyk, A. Alù, D. A. Pawlak, and C. Sibilia, *Adv. Opt. Mater.*, **8**, Iss. 7: 1901617 (2020).
7. K. A. Jackson and J. D. Hunt, *Trans. Metall. Soc. AIME*, **236**: 1129 (1966).
8. M. A. Ivanov and A. Yu. Naumuk, *Metallofiz. Noveishie Tekhnol.*, **36**, No. 12: 1571 (2014) (in Russian).
9. M. Serefoglu, S. Bottin-Rousseau, and S. Akamatsu, *Acta Mater.*, **242**: 118425 (2023).
10. L. Rátkai, G. I. Tóth, L. Környei, T. Pusztai, and L. Gránásy, *J. Mater. Sci.*, **52**: 5544 (2017).
11. A. Gusak and A. Titova, *J. Chem. Phys.*, **158**: 164701 (2023).
12. G. Martin and P. Bellon, *C. R. Phys.*, **9**, Nos. 3–4: 323(2008).
13. P. Bellon and G. Martin, *Phys. Rev. B*, **38**, No. 4: 2570 (1988).
14. P. Pochet, P. Bellon, L. Chaffron, and G. Martin, *Mater. Sci. Forum*, **225**: 207 (1996).
15. A. M. Gusak, T. V. Zaporozhets, Y. O. Lyashenko, S. V. Kornienko, M. O. Pasichnyy, A. S. Shirinyan, *Diffusion-Controlled Solid State Reactions: In Alloys, Thin-Films and Nanosystems* (John Wiley & Sons: 2010).
16. A. Gusak and N. Storozhuk, *Handb. Solid State Diffus.*, **2**: 37 (2017).
17. A. M. Gusak, C. Chen, and K. N.Tu, *Philos. Mag.*, **96**, Iss. 13: 1318 (2016).
18. K. N. Tu and A. M. Gusak, *Scr. Mater.*, **146**: 133 (2018).
19. A. M. Gusak, A. Titova, and Z. Chen, *Acta Mater.*, **261**: 119366 (2023).

20. Z. Erdélyi, M. Pasichnyy, V. Bezpalchuk, J. J. Tomán, B. Gajdics, and A. M. Gusak, *Comput. Phys. Commun.*, **204**: 31 (2016).
21. http://skmf.eu/ for the Basic Information about the Stochastic Kinetic Mean Field Model and Method.
22. V. M. Bezpalchuk, R. Kozubski, and A. M. Gusak, *Usp. Fiz. Met.*, **18**, No. 3: 205 (2017).
23. A. Gusak, T. Zaporozhets, and N. Storozhuk, *J. Chem. Phys.*, **150**, Iss. 17: 174109 (2019).
24. T. V. Zaporozhets, A. Taranovskyy, G. Jáger, A. M. Gusak, Z. Erdélyi, and J. J. Tomán, *Comput. Mater. Sci.*, **171**: 109251 (2020).
25. B. Gajdics, J. J. Tomán, and Z. Erdélyi, *Comput. Phys. Commun.*, **258**: 107609 (2021).
26. B. Gajdics, J. J. Tomán, H. Zapolsky, Z. Erdélyi, and G. Demange, *J. Appl. Phys.*, **126**, Iss. 6: 065106 (2019).
27. G. Jáger, J. J. Tomán, and Z. Erdélyi, *J. Alloys Compd.*, 910: 164781 (2022).